ISSN 1064-2269, Journal of Communications Technology and Electronics, 2013, Vol. 58, No. 2, pp. 110–117. © Pleiades Publishing, Inc., 2013.
Original Russian Text © B.A. Belyaev, A.A. Leksikov, A.M. Serzhantov, V.V. Tyurnev, Ya.F. Bal'va, An.A. Leksikov, 2013, published in Radiotekhnika i Elektronika, 2013, Vol. 58, No. 2, pp. 127–135.

ELECTRODYNAMICS AND WAVE PROPAGATION

Bandpass Filter with an Ultra-Wide Stopband Designed on Miniaturized Coaxial Resonators

B. A. Belyaev[a, b, c], A. A. Leksikov[a, b, c], A. M. Serzhantov[a, b], V. V. Tyurnev[a, b], Ya. F. Bal'va[a, c], and An. A. Leksikov[a]

[a] *Kirensky Institute of Physics, Russian Academy of Sciences, Siberian Branch, Akademgorodok 50, bld. 38, Krasnoyarsk, 660036 Russia*

[b] *Siberian Federal University, ul. Kirenskogo 26, 660074 Russia*

[c] *Siberian State Aerospace University, pr. im. gazety Krasnoyarskii rabochii 31, 660014 Russia*

e-mail: belyaev@iph.krasn.ru

Received February 13, 2012

Abstract—Characteristics of a new miniaturized coaxial resonator are theoretically investigated. It is shown that the first resonant frequency of the resonator can be significantly lowered relative to the second one and the resonator dimensions can be considerably decreased as compared to those of a traditional dielectric-filled quarter-wavelength coaxial resonator. Based on the investigated resonator, a fourth-order bandpass filter has been designed and fabricated. The filter stopband at a level of no worse than −90 dB extends to the frequency that exceeds the passband center frequency by a factor of 47. Calculated frequency responses are in good agreement with those measured on the fabricated filter prototypes.

DOI: 10.1134/S1064226913020022

INTRODUCTION

The advances in wireless communication and radar systems operating at a high noise level require the development of new miniature bandpass filters with improved frequency-selective characteristics. In such devices, it is important to not only lower the level of power transmission in the stopbands above and below the passband, but, simultaneously, broaden the high-frequency stopband. It is well known, however, that the selective properties of filters significantly degrade because of the existence of spurious passbands arising in the regions of resonant frequencies of higher-order oscillation modes of the resonators on which the filters are designed.

In classical microwave filters whose resonators are implemented as half- or quarter-wavelength sections of the transmission line, the second (spurious) passband is located approximately at frequencies of $2f_0$ or $3f_0$, where f_0 is the center frequency of the filter passband. The high-frequency stopband is either narrower or slightly wider than an octave.

There are several ways of broadening the high-frequency stopband and, accordingly, improving the selective properties of a filter. One of these ways is to use stepped impedance resonators. In such resonators, the resonant frequency of the second oscillation mode is multiply higher than the frequency of the first mode. Filters designed on stepped impedance resonators can be both microstrip [1–3] and coaxial [4–6]. However, the high-frequency stopband can be broadened in filters based on resonators with not only stepped impedance but also with smooth variation of the impedance [7].

The passband parameters are also improved by using more complex resonators with either various irregularities, such as loops or interdigital structures [8–10], or defects, such as ground-plane apertures in planar designs [11, 12]. In such designs, the level of microwave power transmitted at higher resonances is lowered, which allows significant broadening of the stopband at a relatively low suppression level in it. For example, in the design proposed in [10], the authors managed to bring the high-frequency edge of the stopband to almost $9.5f_0$, but at an attenuation level in the stopband of only −20 dB. In miniature filters of original designs, where resistive film elements are used to suppress the Q factor of the resonances of higher-order oscillation modes [13, 14], the high-frequency edge of the stopband extends up to $12.5f_0$, now at a level of −30 dB. However, modern communication and radar systems often require not only an extended high-frequency stopband but also much higher suppression of the microwave power in it.

Parameters of the high-frequency stopband of a bandpass filter can be significantly improved by using a new design of the miniaturized coaxial resonator proposed in [15, 16].

In this paper, we analyze such a coaxial resonator and investigate the selective properties of filters based on it. An analogue of the investigated device is a suspended stripline filter with the two-sided pattern of strip conductors [17, 18]. This filter is characterized by better

selective properties as compared to the above filters; however, its characteristics are significantly worse than the characteristics of the filter designed on the investigated coaxial resonators.

1. DESIGN AND CHARACTERISTICS OF THE MINIATURIZED COAXIAL RESONATOR

Figure 1a shows the longitudinal section of the investigated resonator. The base of the resonator is a section of a dielectric tube (*1*) with length l_a, which is made of high-quality ceramic with relative permittivity ε_r. Inner and outer surfaces *2* of the tube are metallized. Cylindrical conductors of the resonator are the coaxial thin-walled metal tubes with radii r_1 (inner) and r_2 (outer). One end of each tube is connected with a wall of metal shielding case *3*, which is a cylinder with diameter r_3; one tube end is connected to the right and the other, to the left end of the case. The other ends of the tube conductors are open-circuited and separated from the end walls of the screen by gap l_1. The cylindrical conductors have an overlap region of length l_3. Note that the inner conductor of the dielectric tube may be a solid rod occupying the entire internal space for length l_2.

When analyzing this design, we will not take into account higher-order modes. Therefore, the equivalent circuit of the resonator (Fig. 1b) contains three sections of two-wire transmission lines that correspond to tree regular resonator sections with lengths l_1, l_2, and l_3 (Fig. 1a). All sections are connected in series; one section (having length l_3) is open-circuited. The electrical lengths and impedances of the sections are θ_1 and Z_1, θ_2 and Z_2, and θ_3 and Z_3, respectively. The transmission-line sections with lengths l_2 (air-filled) and l_3 (dielectric-filled) are uniform; therefore, their fundamental modes are transverse. The line segment of length l_1 has inhomogeneous air–dielectric filling; therefore, its fundamental mode is quasi-transverse.

Effective permittivities ε_n and impedances Z_n ($n = 1, 2, 3$) for fundamental modes in two-wire transmission lines can be calculated from the following formulas, which were obtained in the quasi-static approximation:

$$\varepsilon_1 = \left[\frac{\ln(r_3/r_1)}{\ln(r_2/r_1)/\sqrt{\varepsilon_r} + \ln(r_3/r_2)}\right]^2,$$
$$Z_1 = \frac{1}{2\pi}\sqrt{\frac{\mu_0}{\varepsilon_0}}\left[\frac{\ln(r_2/r_1)}{\sqrt{\varepsilon_r}} + \ln(r_3/r_2)\right], \quad (1)$$

$$\varepsilon_2 = 1, \quad Z_2 = \frac{1}{2\pi}\sqrt{\frac{\mu_0}{\varepsilon_0}}\ln(r_3/r_2), \quad (2)$$

$$\varepsilon_3 = \varepsilon_r, \quad Z_3 = \frac{1}{2\pi}\sqrt{\frac{\mu_0}{\varepsilon_0}}\frac{\ln(r_2/r_1)}{\sqrt{\varepsilon_r}}. \quad (3)$$

From the condition of continuity of currents and voltages at the boundaries of the conductors of all the regular sections of the model, we can easily obtain the equation for the resonant frequencies of the coaxial resonator under consideration:

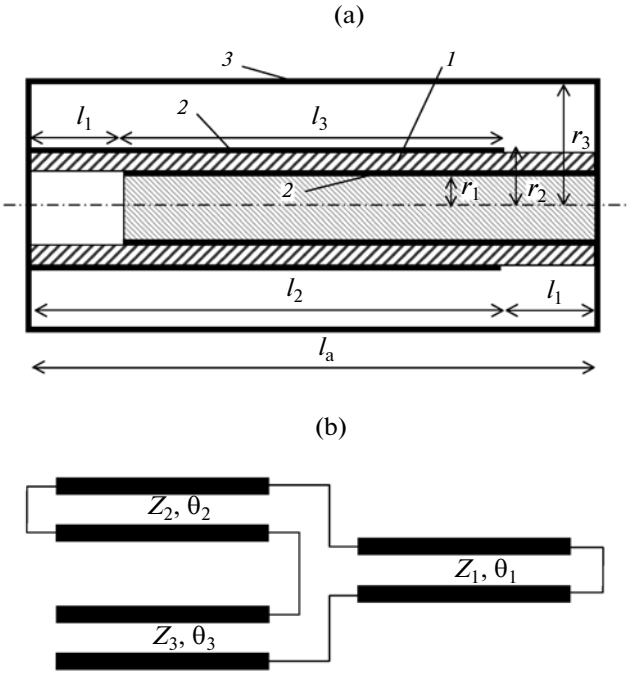

Fig. 1. (a) Design and (b) equivalent circuit of the miniaturized coaxial resonator: (*1*) dielectric tube, (*2*) conductors, and (*3*) metal case.

$$Z_2 \tan\theta_2 + Z_1 \tan\theta_1 - Z_3 \cot\theta_3 = 0. \quad (4)$$

Equation (4) is also valid for damped oscillations. In this case, all its parameters (θ_n and Z_n) are complex and their values can be obtained from real quantities with the use of the following substitutions:

$$\theta_n \to \theta_n\left(1 - \frac{i}{2Q_{0a}} + \frac{i}{2Q_n} + \frac{i}{2Q_d}\right),$$
$$Z_n \to Z_n\left(1 + \frac{i}{2Q_n} - \frac{i}{2Q_d}\right). \quad (5)$$

Here, Q_{0a} is the intrinsic Q factor of the analyzed resonator, which must be found from Eq. (4); Q_n is the Q factor of the conductors of the nth section of the transmission line; and Q_d is the Q factor of the used dielectric material.

In the quasi-static approximation, parameters Q_n are expressed as [19]

$$Q_1 = \frac{2r_3}{\Delta}\frac{\ln(r_3/r_1)}{1 + r_3/r_1}, \quad Q_2 = \frac{2r_3}{\Delta}\frac{\ln(r_3/r_2)}{1 + r_3/r_2},$$
$$Q_3 = \frac{2r_2}{\Delta}\frac{\ln(r_2/r_1)}{1 + r_2/r_1}, \quad (6)$$

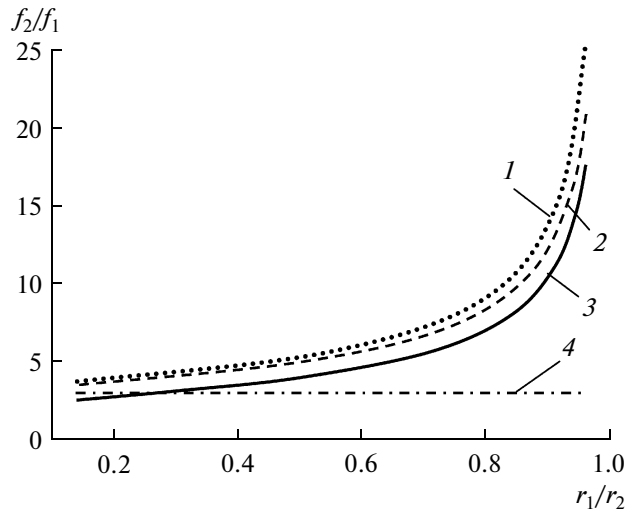

Fig. 2. Dependences of the ratio between the second and first resonant frequencies on the radius of the center conductor normalized to $r_2 = 2.8$ mm for the investigated resonator with $\varepsilon_r = 80$ (*1*), 9.8 (*2*), and 1 (*3*) and (*4*) for the conventional quarter-wavelength coaxial resonator.

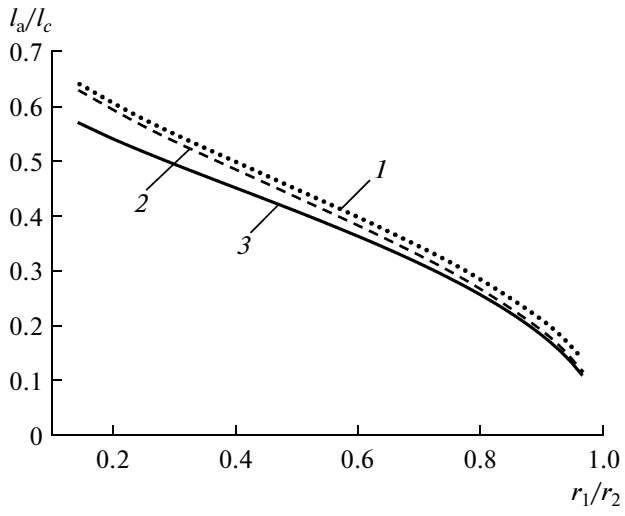

Fig. 3. Dependences of the ratio between the lengths of the miniaturized resonator and the conventional quarter-wavelength coaxial resonator on the normalized radius of the center conductor at $\varepsilon_r = 80$ (*1*), 9.8 (*2*), and 1 (*3*).

where Δ is the depth of the conductor's skin layer. All Q factors in (5) and (6) are assumed to be much higher than unity.

Let us compare the investigated miniaturized coaxial resonator with a conventional quarter-wavelength coaxial resonator filled with the same dielectric. We consider the case when the frequency of the first resonance is fixed at $f_1 = 100$ MHz, assuming for certainty that the radii of the cylindrical shielding cases of both resonators $r_3 = 10$ mm, the radii of the inner conductors $r_2 = 2.8$ mm, and the length of the first section $l_1 = r_2$. It can be easily checked that the chosen ratio r_3/r_2 corresponds to the maximum intrinsic Q factor of a conventional coaxial resonator.

Dependences of the ratio between the second and first resonant frequencies f_2 and f_1 on radius r_1 of the center conductor normalized to the fixed radius $r_2 = 2.8$ mm, which we obtained for the investigated miniaturized resonator, are shown in Fig. 2. Calculation was made for three values of the permittivity of the tube material that correspond to three fillings widely used in microwave technology: TBNS ceramics ($\varepsilon_r = 80$), alumina ($\varepsilon_r = 9.8$), and air ($\varepsilon_r = 1$). The figure shows also the value of the ratio f_2/f_1 for a conventional quarter-wavelength resonator. As is known, this value is independent of filling permittivity and is equal to 3.

Obviously, for any resonator, the ratio f_2/f_1 characterizes the relative width of the high-frequency stopband of the filter designed on its basis. It can be seen in Fig. 2 that, for the investigated resonator, this ratio is always higher than that for a traditional dielectric-filled quarter-wavelength coaxial resonator. This regularity is broken only for the air-filled design in the short initial segment where $r_1/r_2 < 0.3$. In this segment, the ratio f_2/f_1 obtained for the traditional coaxial resonator is noticeably higher. However, for any permittivity of the tube material, the ratio f_2/f_1 rapidly grows with increasing r_1. This fact indicates that, with a decrease in the thickness of the dielectric tube wall, the considered resonator allows multiple broadening of the stopband of the filter based on this resonator as compared to that of the filter based on conventional quarter-wavelength coaxial resonators. In addition, it can be seen that the ratio f_2/f_1 monotonically grows with permittivity ε_r. This increase can be explained by the fact that the stepped impedance of the transmission-line sections forming the resonator increases with increasing ε_r. As is known, this increase leads to an additional lowering of the resonant frequency of the first oscillation mode relative to the frequency of the second mode, analogously to the traditional resonators with stepped impedance [1–6].

Figure 3 shows the dependences of the ratio between length l_a of the analyzed resonator to length l_c of the conventional quarter-wavelength coaxial resonator on radius r_1 of the center conductor normalized to $r_2 = 2.8$ mm. We assume that length l_c of the coaxial resonator is $\lambda_0/\left(4\sqrt{\varepsilon_r}\right) + r_2$, where λ_0 is the wavelength in vacuum. The dependences were calculated again for three above values of permittivity of the ceramic tube. Note that, at the frequency $f_1 = 100$ MHz chosen for certainty, the length of the conventional quarter-wavelength coaxial resonator $l_c = 242.4$, 86.7, and 752.8 mm for alumina ($\varepsilon_r = 9.8$), TBNS ceramic ($\varepsilon_r = 80$), and air fillings, respectively. It can be seen in Fig. 3 that the length of the investigated resonator is initially smaller than that of the coaxial one by 40% and rapidly decreases with increasing r_1. This indicates that the

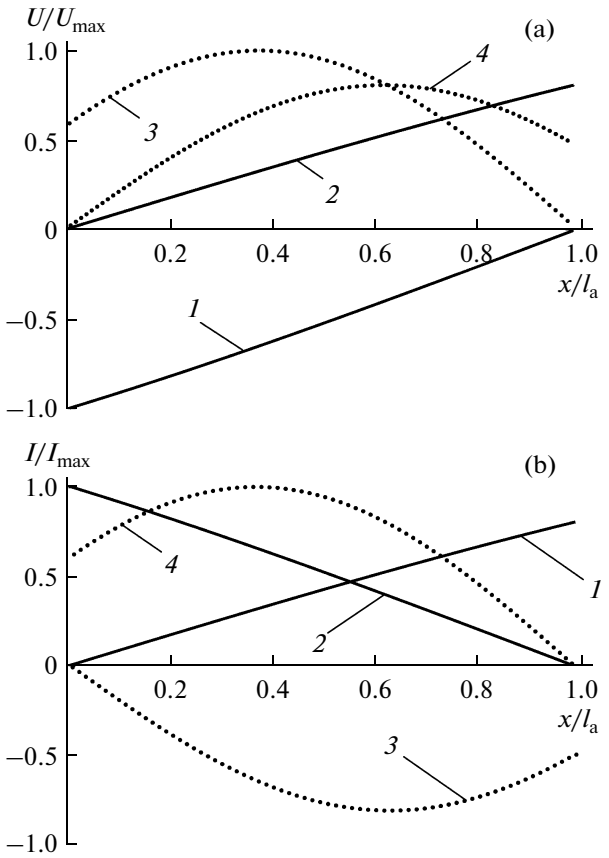

Fig. 4. Distributions of the amplitudes of the high-frequency (a) voltages and (b) currents along the length of the miniaturized resonator on the (*1* and *3*) inner and (*2* and *4*) outer conductors of the dielectric tube for the (solid lines) first and (dots) second resonances.

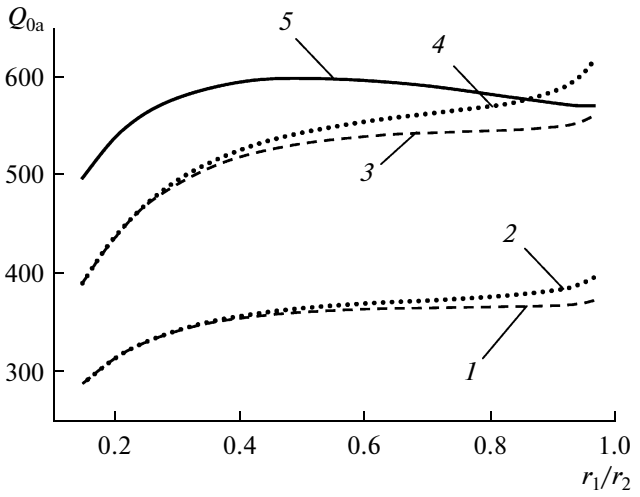

Fig. 5. Dependences of the intrinsic Q factor of the miniaturized resonator for (*1*) $\varepsilon_r = 9.8$, $Q_d = 10^3$; (*2*) $\varepsilon_r = 80$, $Q_d = 10^3$; (*3*) $\varepsilon_r = 9.8$, $Q_d = 10^4$;(*4*) $\varepsilon_r = 80$, $Q_d = 10^4$; and (*5*) $\varepsilon_r = 1$, $Q_d = \infty$.

miniaturization degree l_a/l_c of the resonator grows as the thickness of the dielectric tube wall decreases due to multiple reduction of the resonator length as compared to the length of the conventional quarter-wavelength resonator. It is important that the ratio l_a/l_c depends also on the permittivity of the ceramics. This ratio grows with ε_r as the investigated resonator, in contrast to the conventional coaxial one, is partially filled with a dielectric material. Nevertheless, the length of the investigated resonator at a sufficiently thin wall of the dielectric tube that forms the resonator is smaller than the length of the conventional dielectric-filled quarter-wavelength coaxial resonator by an order of magnitude.

The reason for such a high miniaturization degree of the resonator under consideration becomes evident from the distribution of the amplitudes of high-frequency voltages U and currents I along the resonator length (Fig. 4). The dependences of the amplitudes on coordinate x are plotted at the resonant frequencies of the first (solid lines) and second (dots) oscillation modes for $\varepsilon_r = 1$ and $r_1/r_2 = 0.5$. It can be seen that, for the first resonance, the voltage amplitudes (Fig. 4a) on the inner (*1*) and outer (*2*) conductors of the dielectric tube have opposite signs and vary almost linearly along the resonator length. The dependences of the current amplitudes on these conductors (Fig. 4b) for the first resonance are also linear, but the directions of the currents on the inner (*1*) and outer (*2*) conductors are the same. This fact means that the inner and outer conductors of the dielectric tube can be considered not only as coupled conductors with currents but also as plates of a tubular capacitor whose capacitance is obviously proportional to the permittivity of the tube material and inversely proportional to the thickness of the tube wall.

At the second resonant frequency (curves *3* and *4* in Fig. 4), the voltage amplitudes on the inner and outer conductors of the tube have, on the contrary, the same signs and the currents are opposite. Therefore, at a fixed resonator length, as the thickness of the dielectric-tube wall decreases, the resonant frequency of the first oscillation mode strongly decreases with simultaneous increase in the frequency of the second mode. As a result, the investigated resonator has not only a high ratio between the eigenfrequencies of the second and first oscillation modes as compared to the dielectric-filled quarter-wavelength coaxial resonator but also much smaller dimensions at the same value of the first resonant frequency.

As is known, one of the important characteristics of the resonators is the intrinsic Q factor, which, in particular, determines the loss of the microwave power in the filter passband. Figure 5 shows the dependences of intrinsic Q factor Q_{0a} of the investigated resonator on radius r_1 of the center conductor normalized to the fixed radius $r_2 = 2.8$ mm. The dependences are calculated for the resonators with the tube permittivities $\varepsilon_r = 9.8$ (dashed lines), 80 (dotted lines), and 1 (solid

line). It was assumed that all conductors are made of copper and their thickness exceeds by far the thickness of the skin layer. In this case, at a frequency of 100 MHz, the intrinsic Q factor of the conventional dielectric-filled coaxial resonator $Q_{0c} = 457$ at the Q factor of dielectric $Q_d = 10^3$ and $Q_{0c} = 777$ at $Q_d = 10^4$. This value monotonically grows by more 5% as $Q_d \to \infty$.

It can be seen in the figure that intrinsic Q factor Q_{0a} of the investigated resonator is always lower than intrinsic Q factor Q_{0c} of the conventional coaxial resonator. For the resonators with the tube permittivity $\varepsilon_r > 1$, the intrinsic Q factor monotonically grows with radius r_1 of the center conductor and reaches about 86% of Q_{0c} at $Q_d = 10^3$ and 77% of Q_{0c} at $Q_d = 10^4$. It is noteworthy that, for $\varepsilon_r = 9.8$ and 80, the Q factors of the investigated resonators are almost the same at large thicknesses of the dielectric-tube wall. However, as the thickness decreases, Q_{0a} grows with ε_r (Fig. 5); the thinner the dielectric-tube walls and the higher Q factor Q_d of the tube material, the higher Q_{0a}. However, Q factor Q_{0c} of the traditional coaxial resonator remains invariable, irrespectively of the filling permittivity.

The observed difference in the behavior of $Q_{0a}(r_1/r_2)$ at $\varepsilon_r = 1$ is related to the fact that, in resonators with high permittivity of the tube, the electromagnetic energy is mainly concentrated in the tube volume between the inner and outer conductors, while, in an air-filled resonator, this energy is accumulated in the entire volume of the design, and only at small gaps between the conductors (at $r_1/r_2 \to 1$) the energy is also concentrated in the volume of the thin-walled "air" tube.

2. BANDPASS FILTERS BASED ON MINIATURIZED COAXIAL RESONATORS

To illustrate the potentialities of application of the investigated resonators in fabrication of high-quality miniature bandpass filters, we developed two designs consisting of four electromagnetically coupled coaxial resonators arranged abreast in parallel to each other in a rectangular metal shielding case. The designs have different dimensions and permittivities of the tube materials. Coaxial port connectors with a characteristic impedance of 50 Ω were connected to external cylindrical conductors of input/output resonators of the filters by small tapping wires.

The filters were designed by parametric synthesis in CST Microwave Studio software package with the use of an original method for correction of the design parameters [20]. The method was developed for the synthesis of microstrip filters with specified values of the center frequency, passband width, and return loss level in the passband. Center frequency f_0 of the filter passband was tuned by varying length l_a, common for all resonators (Fig. 1a), and the passband width was tuned by changing distances between resonators. The mean level of return loss maxima in the passband was tuned to a specified level by changing the tapping point position of the input/output resonators. Alignment of the return loss maxima in the passband were tuned by opposite varying l_1 for the external and internal resonators and choosing the distances between the adjacent resonators.

Figure 6 presents the photograph of the operating prototype of the first of the two developed bandpass filters and the frequency response of the device measured on a Rohde & Schwartz ZVK vector analyzer with a dynamic range of 110 dB. In this design, the resonator tubes were made of a ceramics with $\varepsilon_r \approx 50$ and had the following dimensions: $l_a = 17$ mm, $r_1 = 1.7$ mm, and $r_2 = 2.0$ mm and; the internal dimensions of the filter's rectangular case were $67 \times 17 \times 14$ mm^3. The figure shows also the characteristics obtained by means of the electromagnetic numerical analysis of the model of the developed filter. It can be seen that the theory is in good agreement with the experiment. However, the fact that modeling yields the power transmission level in the stopband by 20 dB lower as compared to the experiment is possibly related to an insufficiently high dynamic range of the equipment used. The fabricated filter has the passband center frequency $f_0 = 169$ MHz at an absolute bandwidth measured at a level of −3 dB of $\Delta f = 7.9$ MHz (the fractional bandwidth is 4.7%). The minimum microwave power loss in the filter passband is −2.7 dB at a maximum level of the return loss in the passband of −13.6 dB. The filter stopband at a level of −90 dB extends up to 8 GHz, i. e., to $47f_0$.

Such a wide stopband of the filter cannot be explained by only a high ratio between the resonant frequencies of the second and first oscillation modes, which amounts to $f_2/f_1 \approx 11$ for the resonators used in the filter (because, in these resonators, $r_1/r_2 = 0.85$). Note that the resonance of the second oscillation mode at $f_2 \approx 1870$ MHz is revealed in the calculated frequency response; however, its level is below −140 dB. This fact indicates that, in such a design of the filter, interaction of the resonators at the higher-order oscillation modes is almost absent. At the first oscillation mode, interaction of the resonators is mainly inductive, since almost all energy of the electric field is concentrated in the ceramics inside the resonator. Such an interaction is ensured by high-frequency currents on the outer conductors of the dielectric tube (the distribution of their amplitudes is shown in Fig. 4). At frequencies of the higher-order resonances, the amplitudes of the high-frequency currents and voltages on the outer conductors multiply change their direction along the length of these conductors. Therefore, the integral coefficients of both the inductive and capacitive couplings, are summed at separate parts of the resonators with the opposite signs and approach zero, thus ensuring such a broad stopband of the investigated filter at such a high microwave power suppression level in this band. The spurious passband at fre-

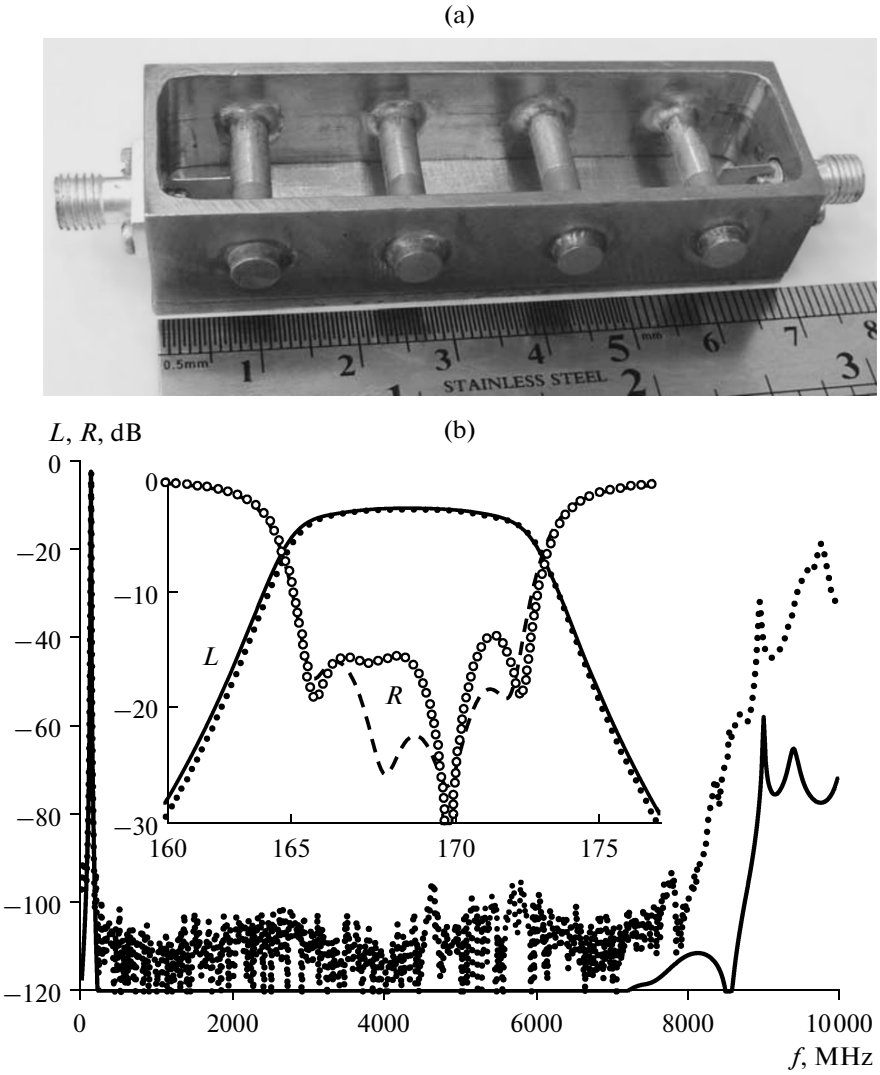

Fig. 6. (a) Photograph of the operating prototype of the filter designed on the miniaturized coaxial resonators with an open top cover and (b) frequency responses of the device for insertion (L) and return (R) losses. The inset shows a fragment of the passband: (lines) calculation and (dots) experiment.

quencies above 8000 MHz is caused by the resonances of the entire filter's internal volume.

Figure 7 presents the photograph of the operating prototype of the second developed filter in which miniaturized resonators have the form of metal rods placed inside thin-walled metal tubes. Each rod is connected with one wall of the case at one end; the opposite ends of the tubes are connected with the other wall of the case. The other ends of the rods and the tubes are open-circuited and are separated from the walls of the case by gap l_1 (Fig. 1a). In essence, the only difference between the resonators in this filter and resonators in the design considered above is that, in these resonators, the walls of dielectric tubes are replaced with air walls ($\varepsilon_r = 1$). The dimensions of the resonators (see the designation in Fig. 1a) are $l_a =$ 22 mm, $r_1 = 1.75$ mm, and $r_2 = 2.0$ mm and the internal size of the filter case is $81.5 \times 22 \times 15$ mm^3.

Figure 7 presents frequency responses of the insertion loss (solid curve) and return loss (dashed line) that were obtained by means of the electromagnetic numerical analysis of a 3D model of the developed filter and corresponding experimental responses (filled and open dots). Similarly to the case of the first filter, the theory is in good agreement with the experiment. The fabricated prototype of the device has the passband center frequency $f_0 = 850$ MHz for an absolute bandwidth at a level of -3 dB, $\Delta f =$ 17.0 MHz (the fractional bandwidth is 2.0%). The minimum insertion loss of microwave power in the filter passband is -2.2 dB at a maximum level of the return loss of -14.2 dB.

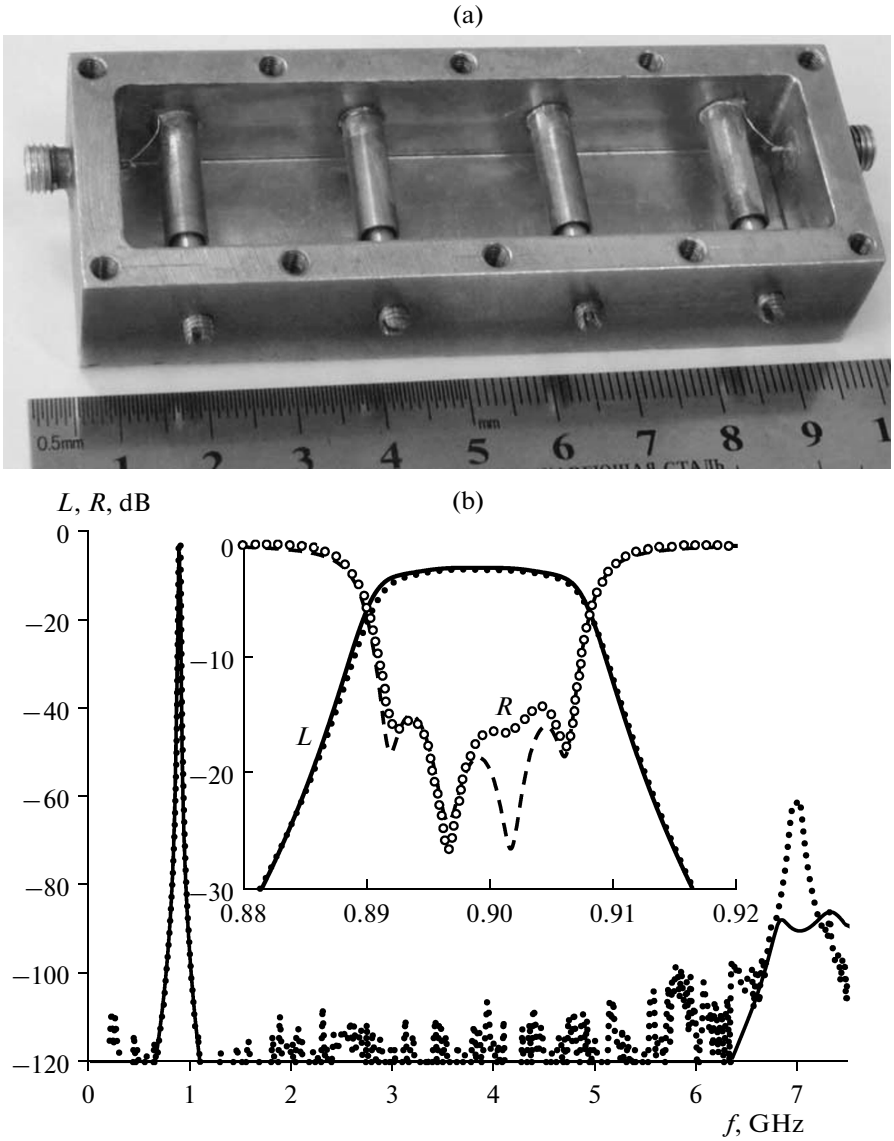

Fig. 7. (a) Photograph of the operating prototype of the filter designed on the miniaturized air-filled coaxial resonators and (b) frequency responses of the device for insertion (L) and return (R) losses. The inset shows a fragment of the passband: (lines) calculation and (dots) experiment.

In this filter, owing to air filling of the resonators, there is no dielectric loss. Therefore, while the fractional bandwidth of the filter is half the fractional bandwidth of the filter with dielectric tubes having relatively low Q factor of the material ($Q_d \approx 400$), the minimum level of the insertion loss in the filter is noticeably lower. However, in the stopband of this filter, there are many spurious passbands with different monotonically decreasing attenuation levels; first of these passbands, with an attenuation of more than 60 dB, is observed at a frequency of ~7 GHz (Fig. 7). These spurious passbands correspond to the resonances of the higher-order oscillations and are caused by weak concentration of high-frequency electric and magnetic fields in the miniaturized coaxial resonators due to small permittivity of air ($\varepsilon_r = 1$). As a result, the filter stopband at a level of –90 dB extends to only 6.4 GHz, i. e., to $7.5f_0$.

Below, we present the positions of the high-frequency edge of the stopband determined at several levels of the minimum attenuation in it.

Attenuation level, dB	Stopband edge
–90	$7.5f_0$
–60	$10.7f_0$
–40	$13.9f_0$
–30	$17.2f_0$

It can be seen that the filter designed on the miniaturized air-filled coaxial resonators has a narrower stopband as compared to that of the investigated filter designed on dielectric tubes; however, it outperforms all known designs based on both the stepped impedance resonators [1–7] and the resonators with resistive film elements used to suppress resonances of higher-order oscillation modes [13, 14].

CONCLUSIONS

Thus, the investigations of a miniaturized coaxial resonator based on a metallized dielectric tube have shown that the resonator length can be many times shorter than the length of a traditional dielectric-filled quarter-wavelength coaxial resonator made of the same material. This length rapidly decreases with decreasing thickness of the ceramic tube wall with simultaneous growth of the intrinsic Q factor of the first oscillation mode of the resonator and the ratio between the frequencies of the second (spurious) resonance and the first operating resonance. This fact allows building the bandpass filters with a record width of the stopband on such resonators.

On the basis of miniaturized coaxial resonators, a fourth-order bandpass filter with the center frequency $f_0 = 169$ MHz, the bandwidth $\Delta f = 7.9$ MHz, and the stopband at a level of –90 dB extending up to 8000 MHz, i. e., to $47f_0$ has been designed. The metal case of the filter has internal dimensions of $67 \times 17 \times 14$ mm^3. The investigated resonators are promising for design of miniature bandpass filters with an ultra-wide stopband and a high rejection in the stopband.

ACKNOWLEDGMENTS

This study was supported by the Special Federal Program "Scientific and Pedagogical Personnel of Innovative Russia" for years 2009–2013 and the Siberian Branch of the Russian Academy of Sciences (integration project nos. 43 and 109).

REFERENCES

1. J.-T. Kuo and E. Shih, IEEE Trans. Microwave Theory Tech. **51**, 1554 (2003).
2. B. A. Belyaev, S. V. Butakov, N. V. Laletin, A. A. Leksikov, V. V. Tyurnev, and O. N. Chesnokov, J. Commun. Technol. Electron. **49**, 1308 (2004).
3. B. A. Belyaev, S. V. Butakov, N. L. Laletin, A. A. Leksikov, V. V. Tyurnev, and O. N. Chesnokov, J. Commun. Technol. Electron. **51**, 20 (2006).
4. M. Sagawa, M. Makimoto, and S. Yamashita, IEEE Trans. Microwave Theory Tech. **33**, 152 (1985).
5. H.-H. Chen, R.-C. Hsieh, Y.-T. Shih, et al., in *Proc. 2010 Asia–Pacific Microwave Conf., Yokohama, Dec. 5–7, 2010* (IEEE, New York, 2010), p. 1724.
6. H.-H. Chen, R.-C. Hsieh, Y.-T. Shih, et al., IET Microwaves, Antennas & Propag. **5**, 459 (2011).
7. B. A. Belyaev, A. A. Leksikov, Yu. G. Shikhov, et al., Elektromagn. Volny Elektron. Sist. **6** (1), 35 (2001).
8. Z. Y. Xiao, S. Gao, D. C. Ma, and L. L. Xiang, Microwave J. **54** (5), 182 (2011).
9. J.-S. Hong and M. J. Lancaster, IEEE Trans. Microwave Theory Tech. **45**, 2358 (1997).
10. G. Zheng and W. Lin, Microwave Opt. Technol. Lett. **52**, 2218 (2010).
11. X. Luo, J.-G. Ma, and E. Li, Microwave Opt. Technol. Lett. **53**, 1786 (2011).
12. M.-H. Weng, H.-W. Wu, Y.-C. Chang, et al., Microwave Opt. Technol. Lett. **49**, 159 (2007).
13. B. A. Belyaev, V. V. Tyurnev, and Yu. G. Shikhov, RF Patent No. 2078393, Byull. Izobret., No. 12 (1997).
14. B. A. Belyaev, S. V. Matveev, V. V. Tyurnev, and Yu. G. Shikhov, Elektron. Tekhnika, Ser. SVCh., No. 4, 20 (1994).
15. B. A. Belyaev, A. M. Serzhantov, V. V. Tyurnev, A. A. Leksikov, and An. A. Leksikov, Tech. Phys. Lett. **38**, 47 (2012).
16. B. A. Belyaev, A. M. Serzhantov, V. V. Tyurnev, and A. A. Leksikov, Microwave Opt. Technol. Lett. **54**, 1117 (2012).
17. B. A. Belyaev, A. A. Leksikov, V. V. Tyurnev, and A. V. Kazakov, RF Patent No. 2237320, Byull. Izobret., No. 27 (2004).
18. B. A. Belyaev, A. M. Serzhantov, and A. A. Leksikov, J. Commun. Technol. Electron. **55**, 1330 (2010).
19. V. V. Tyurnev, *Theory of Microwave Circuits* (IPTs KGTU, Krasnoyarsk, 2003) [in Russian].
20. B. A. Belyaev and V. V. Tyurnev, Izv. Vyssh. Uchebn. Zaved., Fiz. **49** (9), Supplement, 164 (2006).